Proposal of an Experiment for Discovery and Study of Diffracted Radiation of Channeled Electrons

D. A. Baklanov[a], I. E. Vnukov[a], V. K. Grishin[b], A. N. Ermakov[b], Yu. V. Zhandarmov[a], and R. A. Shatokhin[a]

[a] *Belgorod State University, Belgorod, 308015 Russia*

e-mail: vnukov@bsu.edu.ru

[b] *Skobeltsyn Institute of Nuclear Physics, Moscow State University, Moscow, 119991 Russia*

Abstract—It is discussed whether it is possible to discover the diffracted radiation of channeled electrons experimentally. A new method for orienting a crystal in average-energy electron accelerators with short times of the acceleration cycle and the electron spill to the target (microtrons and linear accelerators) is proposed. It uses the integral characteristics of the yield of soft radiation from thin metal targets and provides a considerable decrease in the time required for the crystal orientation. An experimental setup is created, a complex of programs for equipment operation is developed and debugged, and test measurements are conducted at the microtron operating at the Institute of Nuclear Physics of Moscow State University, which makes it possible to carry out proposed experimental studies in the nearest future.

INTRODUCTION

Diffracted radiation of channeled electrons (diffracted channeling radiation, or DCR), or, as it is sometimes referred to, diffracted (diffraction) radiation of a relativistic oscillator (DRO) [1–3], is one of the interesting physical phenomena occurring during the propagation of fast charged particles through ordered media and was predicted by Baryshevskii and colleagues in the 1970s and 1980s. Some of them—for example, parametric X-ray radiation (PXR) of fast charged particles in crystals and PXR at small angles with respect to the direction of the particle velocity—were recorded experimentally [4, 5].

DRO is a result of the coherent summation of two processes, namely, photon radiation and diffraction in crystals [1–3, 6], and has not been studied by experimenters until now, because the size of the effect was insufficiently clear and it was difficult to separate this effect from competing processes, namely, PXR and diffracted bremsstrahlung (DBS). Additional difficulties in studies made to discover this effect include a limited range of particle energies where it is possible to observe this effect clearly (10–40 MeV) and a very narrow range of observation angles and photon energies where this effect can manifest itself distinctly, which imposes rigid requirements on the choice of observation angles and radiation collimation [7].

Recently, after a series of papers were published [7–10], it became clear how to estimate the size of the effect. According to the results of the cited papers, the yield of diffracted radiation of channeled particles can exceed that of PXR by several orders of magnitude in a narrow angular range. If this estimate is valid, we can hope that a new intense X-ray radiation source with readjustable energies can be created, because the radiation source based on the PXR mechanism in perfect crystals was not applicable in practice [11]. The statement of the authors of [6] that the mechanisms of channeling radiation and PXR can interfere is also interesting. In this case, if the diffraction conditions for photons emitted during the transition of electrons from one coupled state to another are satisfied, it is possible to expect a change in the ratio of peaks in the channeling radiation spectrum. Because the interference of coherent bremsstrahlung and channeling radiation was observed experimentally [12, 13], the registration of the effect of the interference of the channeling radiation and PXR mechanisms is an interesting physical problem. It is clear from the preceding that experimental studies conducted to verify theoretical predictions of the DRO size and characteristics are undoubtedly important.

STATEMENT OF THE PROBLEM

According to theoretical predictions [7–10], the effect under discussion can manifests itself almost for any observation angles and, accordingly, for any photon energies under the condition $\omega_B \leq \omega_{ch}$, where ω_{ch} is the channeling radiation photon energy and ω_B is the Bragg energy for the same observation angle. However, the character and the degree of manifestation of this effect depend cardinally on the ratio of these energies. If the Bragg energy is close to the

energy of any peak in the channeling radiation spectrum, then a maximum with an amplitude several times greater than the PXR yield must be observed instead of a minimum at the center of the PXR angular distribution [10].

If this condition is not satisfied, then narrow ring-like structures consisting of two closely located peaks with amplitudes noticeably exceeding the PXR yield appear in the PXR angular distribution. The center of these rings coincides with that of the PXR angular distribution, and their number is determined by the number of peaks in the channeling radiation spectrum [7, 10]. In this case, for the energy $E_0 > 20$–30 MeV of electrons the channeling radiation spectrum of which contains several peaks, an increase in the intensity for all points in the angular distribution or the orientation dependence of the PXR yield can be expected in measurements of the angular distribution or the orientation dependence of the radiation yield using a detector with a finite angular aperture.

As was mentioned in the Introduction, the radiation mechanism was not examined purposefully. The experiment in [14] for an electron energy of 900 MeV and an observation angle of 90°($\omega_B \sim 7$–20 keV), in which the presence of the regime of planar and axial channeling was controlled, showed that there is no channeling effect on the spectrum and the PXR angular distribution. Probably, this is due to a large difference between the typical channeling radiation energy ($\omega_{ch} \sim 3$–5 MeV) and the Bragg energy [7]. PXR experimenters do not usually control whether the channeling regime is fulfilled; moreover, they often use crystals with thicknesses that are much larger than the dechanneling length (~2–10 μm for electron energies less than 100 MeV) required for the effect to be noticeable [7].

However, analysis of the published experimental data shows that this effect could be recorded in some experiments. The authors of [15] reported that the recorded radiation yield from thin silicon and diamond crystals for an observation angle of 180° was twice that predicted by PXR kinematics theory. Because this observation angle for the strictly Bragg orientation corresponds to the normal incidence of electrons on the crystal plane and the crystal targets are usually cut and located so that their faces are parallel to crystallographic planes, it is not excluded that the orientation dependences of the PXR yield obtained in the case where crystals were rotated about the vertical axis were measured under channeling conditions in the horizontal plane.

The condition $\omega_{ch} \sim 20$–100 keV $>> \omega_B \sim 2$–5 keV is satisfied for the electron energy ranging from 30 to 87 MeV and this observation angle; therefore, the discussed effect could manifest itself in an increase in the intensity of the recorded radiation, which was observed in the cited paper, the authors of which explained this increase by the contribution of dynamic effects characteristic to the reflection of X-ray radiation in the Bragg geometry; this explanation seems to us to be wrong, because a significant increase in the PXR intensity (compared to the theoretical predictions) was not observed in other experiments also conducted in the Bragg geometry [14, 16].

The authors of [17] measured the orientation dependence of the PXR yield for the (111) reflection in the Si crystal with a thickness of 17 μm. The measurement geometry was chosen such that the orientation dependences were measured for the electron motion at small angles to the (112) plane. The results of these experiments are interesting, because there was no discrepancy from the predictions of PXR kinematics theory for $E_0 =$ 15.7 MeV. In the case of $E_0 = 25.7$ MeV where the (112)-plane channeling radiation energy is greater than the photon energy for first-order reflection under the conditions of the cited paper (10–15 keV), the recorded radiation yield at all points of the measured orientation dependence turned out to be larger by 30% than that predicted by PXR theory.

It follows from our analysis that the discussed effect probably exists; however, to identify it with confidence, the measurements must be made for thin crystals and under experimental conditions (electron energies and observation angles) such that the Bragg energy be close to the energy of at least one peak in the channeling radiation spectrum. The photon energy range of 20 to 40 keV seems to be most attractive from the methodological point of view. Because the absorption of photons with these energies in the air is low, experiments can be carried out without evacuating the photon propagation path and detectors must be located at large distances from the accelerator in order to decrease the background. This energy range is also interesting from the standpoint of possible practical applications, for example, in medicine, where sources of monochromatic X-ray radiation with photon energies on the order of 20 keV and ranging from 30 to 40 keV are required for mammography and angiography at the edge of the iodine and xenon photoabsorption band [18].

This photon energy range corresponds to channeling of electrons with $E_0 = 20$–30 MeV in diamond and silicon crystals most often used in the experiments conducted to study radiation generation during the fast-particle–crystal interaction. To single out the effect with confidence, it is necessary to satisfy the condition $\upsilon_e \ll \psi_L$, where υ_e and ψ_L are the respective spread of the electron beam at the crystal input and critical angle of planar channeling (ψ_L ~2–3 mrad depends on the electron energy and the crystal used), and to provide conditions for operations with thin crystals [7]. Using a microtron to conduct such an experiment seems to be most preferable from the standpoint of these requirements. The electron beam of a linear accelerator has an overly large spread and variations in the electron energies $\Delta E/E$. For example, $\upsilon_e \sim 1$ mrad and $\Delta E/E \sim 0.5$–1% at the LUE-40 accelerator [17] in the energy range of 15–25 MeV. It is very

difficult to provide single propagation of electrons through a thin target if a betatron is used [19]. The output of the beam from the betatron and the parallel transport of the electron beam of the linear accelerator [20] require a significant complication of the experimental setup.

Therefore, it was assumed that the experiment must be conducted using a split microtron (operating in the Institute of Nuclear Physics of the Moscow State University [21]) with a current of ~3 mA (~10^{12} particles per acceleration cycle), a frequency of 10 Hz, the duration of the radiation cycle $\tau \sim 8$–10 μs, and $\Delta E/E \sim 0.2\%$. For a beam size of 5×5 mm, an emittance of ~1 mm · mrad provides the spread of the electron beam $\upsilon_e \sim 0.2$ mrad. The presence of the led-out electron beam, the required energy range (14.6–67.4 MeV), and the possibility of changing the particle energy make it possible to hope that this type of radiation can be separated from PXR and DBS successfully.

It follows from the experiment simplicity conditions that the channeling plane must coincide with the horizontal one and the plane on which the diffraction of channeling radiation occurs is rotated through a required angle about the vertical axis. To record the desired radiation, it was decided to use X-ray NaI detectors (the practice showed that, for photon energies larger than 20 keV, their resolution is quite sufficient to separate PXR from a continuous background) or a Si pin detector.

To single out the desired effect, it was planned to measure the angle distributions of the X-ray yield for several orders of reflection. If the condition $\omega_{ch} \sim \omega_B$ is satisfied for some order of reflection and a peak in the channeling radiation spectrum, a narrow maximum with a large amplitude must appear at the center of the PXR angular distribution for this order of reflection. Because the probability that this condition is satisfied for other orders of reflection is low, only a slight change in the radiation yield can be observed and the shape of the angular distribution coincides with that predicted by PXR theory in the case of other orders of reflection.

Conducting the same measurements for another electron energy is a control test. All conditions for PXR and DBS generation change sufficiently insignificantly, while there is no coincidence of energies of channeling radiation and diffracted electrons that is required for the desired effect to manifest itself. Therefore, the shape of the angular distribution must coincide with that predicted by PXR kinematics theory. The measurement of spectra for several orders of reflection can yield the same information. The ratio of the radiation yields for different orders of reflection must change in the presence of the desired effect.

To observe the effect, it is necessary to orient the crystal plane along the direction of the electron beam, i.e., to operate in the planar channeling regime. Methods for orienting crystals along the channeling radiation direction by means of a ionization chamber [22] or a NaI (Tl) detector in the Compton geometry [23] that are usually used in higher energy accelerators for electrons with energies of several ten megaelectronvolts are appropriate, because the typical radiation energy for the channeling of such particles does not exceed 50–100 keV.

It is ineffective to use the counting regime of the detector operation that is usually applied to low- and middle-energy accelerators [24] with short times of the acceleration cycle, because the typical pulse duration of the radiation detector (~1–6 μs is comparable with the duration of the acceleration cycle (6–10 μs). Therefore, to exclude superposition, the accelerator current must be maintained so that at most 0.2–0.4 pulses can be recorded during one acceleration cycle [17].

To obtain statistical error on a level of 5% for an accelerator frequency of 10 Hz, at least 100–200 s are required for each crystal orientation. Several orientation dependences with a number of points ranging from 100 to 200 are usually measured during the process of crystal orientation. In other words, the crystal orientation requires 10–20 h of continuous accelerator operation. The orientation using radiation spectra requires a severalfold increase in the operation time and cannot therefore be used in the stage of the initial crystal orientation too. It should be mentioned that it is necessary to measure currents on a level of 10^3–10^5 particles per acceleration cycle during the orientation process using the counting regime of the detector operation, which is a separate technical problem.

The traditional method for orienting crystals by means of thin- and thick-wall ionization chambers [22] (the integral regime of the detector operation is used in this case) is inappropriate for middle-energy electrons because of the low energy of channeling radiation photons. Therefore, to orient crystals, we propose to use an X-ray NaI detector with a thickness of 1 mm located at an angle of 90° and recording a change in the yield of characteristic X-ray radiation (CXR) from a thin metal target inserted in the γ-beam path as a function of the crystal orientation. Such an orientation method in the counting regime was used under the conditions of the acceleration hall of the Tomsk synchrotron for the 500-Mev energy of electrons and demonstrated a good sensitivity [25]. The optimal signal–background ratio can be reached and a change in the intensities of various lines in the spectrum of the radiation under study can be singled out by changing a scatterer. It is decided to conduct measurements in the current regime of the detector operation. This makes it possible to operate in the regime typical of accelerators and decrease the time required to orient crystals.

SIMULATION

To verify the applicability of the proposed method for orienting crystals for smaller electron energies and of a method for obtaining information different from

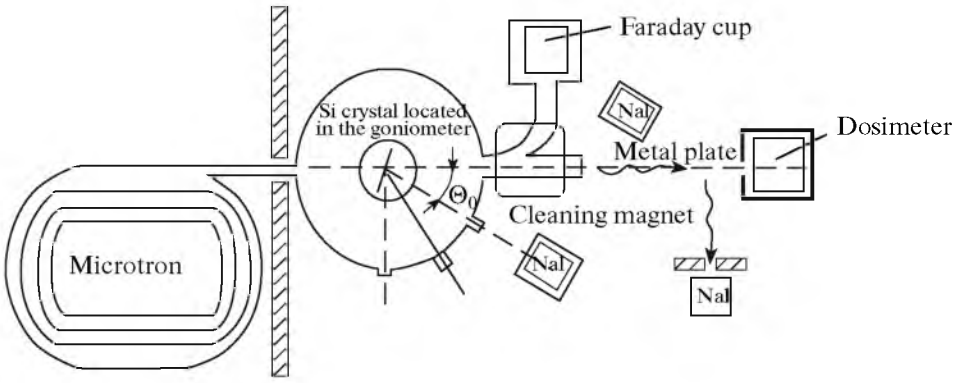

Fig. 1. Scheme of experimental equipment arrangement.

that used in the experiment in [25], we simulate the dependence of the integral response of the detector, i.e., the energy absorbed in the detector, on the spectrum of the analyzed radiation and the target material and the thickness.

We present the main steps and approximations used in the simulation process. A thin parallel beam of γ radiation with the spectrum $N(\omega)$ obtained during the interaction of electrons with the energy E_0 and the crystal is incident on a thin target rotated through an angle of 45° (Fig.1). The target is divided into layers with the thickness $\Delta t \ll l_{abs}$, where l_{abs}, is the absorption length for photons with the energy $\omega_{min} = 10$ keV. The chosen threshold energy is due to strong absorption of lower-energy photons in the air and material of a bremsstrahlung target. The spectrum of photons after the ith layer is determined by the spectrum of radiation incident on it and by the absorption of photons in it:

$$N^i(\omega) = N^{i-1}(\omega)[1 - \sigma_{tot}(\omega)n\Delta t], \quad (1)$$

where n is the concentration of atoms in the target and $\sigma_{tot}(\omega)$ is the cross section for the interaction of photons with the energy ω and target atoms;

$$\sigma_{tot}(\omega) = \sigma_{ph}(\omega) + \sigma_{comp}(\omega) + \sigma_{coh}(\omega) + \sigma_{pair}(\omega), \quad (2)$$

where $\sigma_{ph}(\omega)$, $\sigma_{comp}(\omega)$, $\sigma_{coh}(\omega)$, and $\sigma_{pair}(\omega)$ are the respective cross sections of the processes of photoeffect, Compton and coherent scattering, and creation of electron–positron pairs. The values of the cross sections given in [26] were used in the calculation.

We assumed that CXR photons after the process of photoabsorption by the K shell and photons subjected to coherent and incoherent scattering in the target enter the detector located in the air at a distance of 1m from the target at an angle of 90° with respect to the direction of photon beam incidence on the target. For the materials of interest to us, photons of the L series cannot reach the detector because of absorption in the air and target material. Bremsstrahlung of secondary charged particles and scattering of secondary photons were not taken into account because of the small target thicknesses used.

The number $\Delta N^i(\omega')$ of photons outgoing from the ith layer in the detector direction and their energy ω' were determined by the spectrum of photons reaching this depth, by the processes causing the creation of these photons, by the angular distributions of scattered radiation for each included process, and by the angles of detector location and radiation collimation. The number $\Delta N^i_D(\omega')$ of photons reaching the detector depends on the absorption in the target material and the air along the path from the creation point to the detector:

$$\Delta N^i_D(\omega') = \Delta N^i(\omega')\exp[-\mu_1(\omega')t_1 + \mu_2(\omega')t_2], \quad (3)$$

where $\mu_1(\omega')$ and $\mu_2(\omega')$ are the respective linear absorption coefficients of photons with the energy ω' in the target material and the air and t_1 and t_2 are the respective path lengths in the target and the air.

It was assumed that the distribution $\frac{dN_{ph}(\omega')}{d\Omega}$ of the ejection angles of the CXR photons is isotropic and the cross section s_{ph} of the photoabsorption by the K shell is $\sigma^K_{ph}(\omega) \sim 0.8\sigma^{tot}_{ph}(\omega)$ [27], where $\sigma^{tot}_{ph}(\omega)$ is the cross section of the photoabsorption of the quanta with the same energy [26]. The probabilities of the Auger effect and radiation of photons of the K_α and K_β lines after the photoeffect in the K shell for each material of interest to us were taken into account according to the data given in [28]:

$$\Delta N^i_{ph}(\omega', \omega) = \frac{W\Delta N^i(\omega)\sigma^K_{ph}(\omega)}{\sigma_{tot}(\omega)} \int_{\Delta\Omega} \frac{dN(\omega')}{d\Omega} d\Omega, \quad (4)$$

where W is the probability of the radiation of the CXR quantum after the photoeffect in the K shell, $\Delta\Omega$ is the solid angle overlapped by the collimator with a radiation collimation angle of 2°, and $\Delta N^i(\omega) = N^i(\omega) - N^{i-1}(\omega)$ is the number of primary-beam photons subjected to interaction in the ith layer.

For photons with the energy ω subjected to coherent scattering in the target and outgoing with the same energy in the target direction, we can write

$$\Delta N^i_{coh}(\omega) = \frac{Z\Delta N^i(\omega)\sigma_{coh}(\omega)}{\sigma_{tot}(\omega)\sigma^{calc}_{coh}} \int_{\Delta\Omega} \frac{d\sigma_{coh}}{d\Omega} d\Omega. \quad (5)$$

Here, $\frac{d\sigma_{coh}}{d\Omega}$ and σ_{coh}^{calc} are the respective differential and total cross sections of coherent scattering by a free electron (the Thomson cross section) and Z is the atomic number of the target material,

$$\frac{d\sigma_{coh}}{d\Omega} = \frac{r_e^2}{2}(1+\cos^2\theta), \quad (6)$$

where r_e is the classical electron radius and θ is the photon scattering angle.

For photons with the energy ω subjected to Compton scattering in the target and outgoing with the energy ω' in the detector direction, we can write

$$\Delta N_{comp}^{l}(\omega',\omega) = \frac{Z\Delta N^{l}(\omega)\sigma_{comp}(\omega)}{\sigma_{tot}(\omega)\sigma_{comp}^{calc}(\omega)} \int_{\Delta\Omega} \frac{d\sigma_{comp}(\omega)}{d\Omega} d\Omega. \quad (7)$$

Here, $\frac{d\sigma_{comp}(\omega)}{d\Omega}$ and $\sigma_{coh}^{calc}(\omega)$ are the respective differential and total cross sections of the Compton scattering by a free electron (the Klein–Nishina–Tamm cross section):

$$\frac{d\sigma_{comp}(\omega)}{d\Omega} = \frac{r_e^2}{2}\left(\frac{\omega'}{\omega}\right)^2\left(\frac{\omega}{\omega'} + \frac{\omega'}{\omega} - \sin^2\theta\right), \quad (8)$$

where ω' is the energy of the scattered photon:

$$\omega' = \frac{\omega}{1+\omega(1-\cos\theta)/m_e c^2}. \quad (9)$$

Because the collimation angle of the scattered radiation is small, the dependence of the scattered radiation energy on the ejection angle was not taken into account. With the introduced notation and our assumption taken into account, the integral signal of the NaI(Tl) detector for the target with the thickness T is

$$Y = \int_{\omega_{min}}^{E_0} \omega' f_E(\omega') d\omega' \int_0^T dt \int_{\omega_{min}}^{E_0} (\Delta N_{coh,D}(\omega',t,\omega) + \Delta N_{ph,D}(\omega',t,\omega) + \Delta N_{comp,D}(\omega',t,\omega)) d\omega. \quad (10)$$

Here, $f_E(\omega')$ is the energetic efficiency of the detector,

$$f_E(\omega') = f(\omega')\overline{E}/\omega',$$

where $f(\omega')$ is the detector efficiency and $\overline{E}$ is the average energy left by the photon with the energy ω' in the detector. The dependence of these quantities for the X-ray NaI(Tl) detector with a diameter of 40 mm and a thickness of 1 mm on the photon energy was calculated using the Monte Carlo method according to the procedure given in [29].

To determine the sensitivity of the proposed crystal orientation procedure to the spectrum of the radiation incident on the target, we used the result of the experiment [20] on the (110)-plane 30-MeV electron channeling radiation in the Si crystal with a thickness of 15 μm. Figure 2 shows the initial portions of the radiation spectra used in the simulation. The model channeling radiation spectrum (curve *1*) reproduces the experimental spectrum [20] with an error of at most 30%. The bremsstrahlung spectrum (curve *2*) is calculated using the spectral angular Schiff distribution [30]

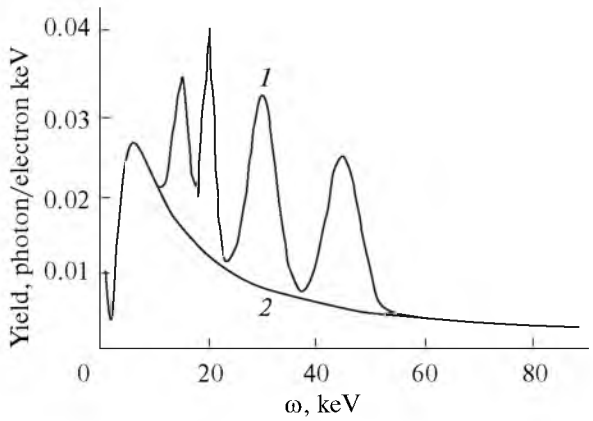

Fig. 2. Radiation spectra of electrons with $E_0 = 30$ MeV in the Si crystal under the experimental conditions [20]: (*1*) (110)-plane channeling radiation and (*2*) bremsstrahlung.

with the initial spread of the electron beam, multiple particle scattering in the crystal, and the radiation collimation angle (0.5 mrad) taken into account. The total number of photons in the channeling radiation spectrum is larger by 25–30% than that in the spectrum of bremsstrahling from the disoriented crystal.

According to the calculated results, the process of photoabsorption of primary-beam quanta in the target makes the main contribution to the recorded radiation yield. The contribution of photons subjected to coherent and incoherent scattering in the target does not exceed fractions of percent for all targets, which is due to both the small cross section and target thicknesses and a low detector efficiency with such a thickness for photon energies $\omega > 100$ keV.

The calculation was carried out for targets made of lead, tin, silver, molybdenum, niobium, and copper, i.e., widely used materials that can be used to prepare foils. Figure 3 shows the dependence of the integral signal from the NaI(Tl) detector on the target thickness for several materials and different radiation spectra. The odd curves correspond to the registration of channeling radiation, and the even curves to that of bremsstrahlung. As can be seen from this figure, materials with larger Z provide a larger response because of a larger energy of CXR photons and a lower probability of the Auger electron emission. At the same time, the distinction between the responses for the spectra of channeling radiation and bremsstrahlung (which is very important from the standpoint of the efficiency of the developed method for orienting crystals) is maximum for materials with an average Z (tin and silver, Fig. 5). It should be mentioned that the recorded radiation has a saturation region for the target thicknesses ranging from 40 to 80 μm, which is due to a large photoabsorption cross section in the energy range of 15–50 keV and due to the absorption of the CXR photons in the target material.

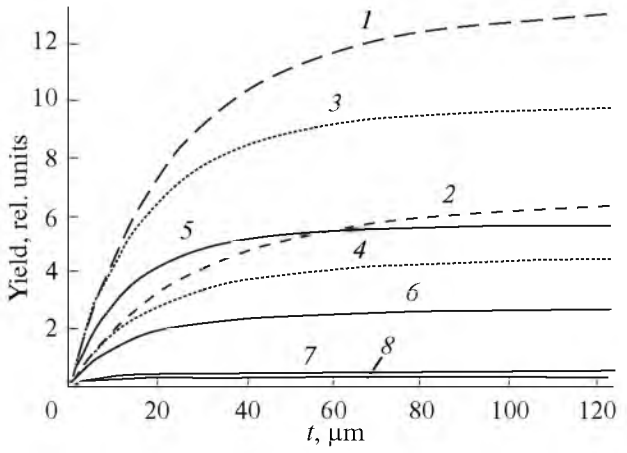

Fig. 3. Dependence of the response of the scattered radiation detector on the spectrum of radiation hitting the target and on the target material and thickness: (*1*) and (*2*) tin, (*3*) and (*4*) silver, (*5*) and (*6*) niobium, and (*7*) and (*8*) copper.

Figure 4 shows the dependence of the ratio of the recorded radiation yields for the spectra of channeling radiation and bremsstrahlung and the lead, tin, silver, niobium, and copper targets (Figs. 1–5). It can be seen from this figure that silver and tin targets are best for implementing the proposed crystal orientation method using the integral yields. Materials with a small Z are worse because of a small response and a small increase in it (Fig. 3), which leads to an increase in the background fraction. Materials with a large Z (lead) are not suitable despite the large response. Because of a large energy threshold of photoabsorption by the K shell (~88 keV) exceeding the spectral channeling radiation region (Fig. 2), the escape of CXR photons from the K shell is independent of the crystal orientation. The difference between the yields of the scattered radiation for this target and the coherent and incoherent radiation spectra is due to the photoabsorption by the L shell. For targets with optimal thicknesses, the ratio of the recorded yields of scattered radiation for the analyzed spectra is ~2.2, which is considerably higher than the ratio of the numbers of photons in these spectra (~1.3).

A sufficiently high sensitivity of the proposed method and the threshold character of the dependence of the photoabsorption cross section on the photon energy make it possible to verify without spectral measurements whether there interference of the PXR and channeling radiation mechanisms exists if the diffraction conditions are satisfied for photons of various peaks in the radiation spectrum. For definiteness, we take a Si crystal with the ⟨111⟩ orientation and 30-MeV electrons. The (110) plane coincides with the horizontal plane, and the (112) plane with the vertical one. According to [20] (Fig. 2), four pronounced peaks with energies of 45, 29.2, 19.7, and 13.6 keV are observed in the (110)-plane channeling radiation spectrum under these conditions.

For the ⟨111⟩ orientation and the chosen geometry of the crystal plane arrangement, the most strong reflection must be observed in the (112) plane (224 reflection) and two planes of the {110} type (220 reflection) rotated through angles of $\pm 30°$ about the vertical plane [5]. If the desired effect exists, then some special features in the (110)-plane channeling radiation spectra must be observed for the angles of crystal axis disorientation along the (110) plane: Θ = 82.9 and 124.6 mrad (ω = 45 keV), Θ = 127.9 and 192.2 mrad (ω = 29.2 keV), Θ = 192 and 287.8 mrad (ω = 19.7 keV), and Θ = 277 and 424.6 mrad (ω = 13.6 keV). The first value of the disorientation angle corresponds to the fulfillment of the Bragg condition for photons in the

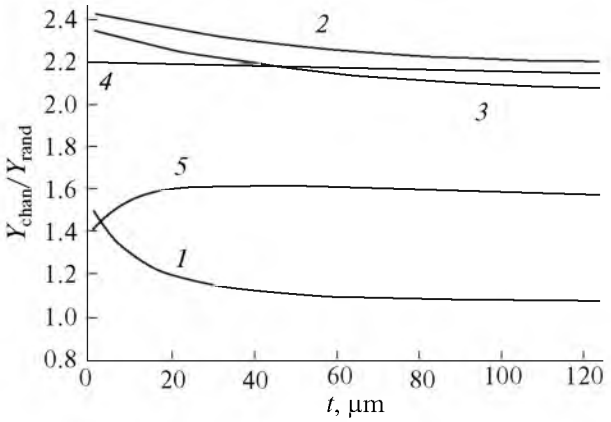

Fig. 4. Dependence of the ratio of the detector response to the radiation with different spectral compositions on the material and thickness of the metal target: (*1*) lead, (*2*) tin, (*3*) silver, (*4*) niobium, and (*5*) copper.

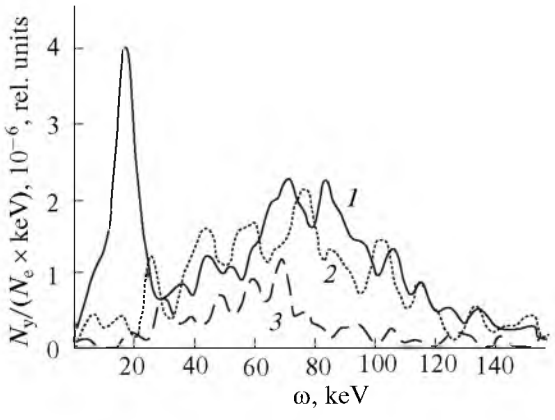

Fig. 5. Radiation spectra for the Nb target: (*1*) the spectrum for the experiment with target, (*2*) the spectrum for the experiment without target, and (*3*) the scattering radiation path blocked by lead with a thickness of 1 mm.

(110) planes, and the second, in the (112) plane. In other words, in the case of the interference of these radiation mechanisms during the measurement of the orientation dependence of the scattered radiation yield along the (110) plane for these angles of axis disorientation, the yield of the recorded radiation must change.

The threshold of photoabsorption by the K shell is 29.2 keV for tin, 25.51 keV for silver, 18.99 keV for niobium, and 8.98 keV for copper; therefore, changes in the spectra due to the fulfillment of the diffraction conditions manifest themselves differently in the measurement of the orientation dependences using thin foils made of these materials. For example, a thin niobium target must be most sensitive to a change in the intensity of the peak with $\omega = 19.7$ keV, while a change in the intensity of this peak does not affect the recorded radiation yield for tin and silver targets.

As the crystal thickness and the radiation collimation angle increase, the ratio of the intensities of the channeling radiation and bremsstrahlung components decreases. Nevertheless, the ratio of the recorded radiation yields for the spectra of channeling radiation and bremsstrahlung remains ~1.1 for a crystal thickness of 0.2 mm and the same collimation angle (0.5 mrad) under the condition that channeling occurs only in a near-surface crystal layer with a thickness less than 0.015 mm. If the effect of the volume capture of electrons in the planar channeling regime at the crystal depth is taken into account [31], this ratio must be slightly better, which makes it possible to hope that the discussed effect can be recorded successfully as the crystal thickness or the radiation collimation angle increase.

EXPERIMENTAL PROCEDIRE AND PRELIMINARY RESULTS

The scheme of our experiment is given in Fig. 1. Electrons led out from the fifth or sixth microtron orbits ($E_0 = 25.2$ or 30 MeV) are inserted into a scattering chamber, where a triple-axis goniometer with a crystal installed in it is located and there are several windows for the radiation output. The operating ranges of the angles Θ_υ and Θ_h of crystal rotation about the vertical and horizontal axes are $\pm 45°$ and $\pm 8°$, respectively. The rotation step is 0.01°. The range of the angles φ of rotation of the electron beam about the axis is $\pm 5°$ with a step of 0.04°. To rotate the goniometer, we used a scheme controlling step motors by means of an LTP computer port; this scheme was proposed in [32] and makes it possible for the motor to operate automatically in the holding current regime in the absence of rotation, which is worthwhile from the standpoint of the goniometer operation in a vacuum, where the heating of motors due to a vacuum deterioration is inadmissible.

The led-out electron beam is measured by either a magneto-inductive sensor in the large current regime or a secondary-emission monitor in the regime of spectral measurements. Electrons passed through the crystal are directed by a cleaning magnet to a "burial." A Faraday cup used to calibrate the secondary-emission sensor can be located there. The main problem to be solved is that, until recently, the accelerator was used to study nuclear reaction cross sections; in this case, it is not necessary to measure currents precisely in each acceleration cycle and there are no sensors measuring small currents. This part of the equipment is now developed and partially adjusted.

The main problem of the first step of measurements was to verify the developed method for orienting crystals in the middle-energy accelerators with short acceleration cycles using the integral scattered radiation yield from a target located in the beam path of the γ radiation beam from the crystal. Because there was no scattering chamber, the experiment was conducted in the air without rotating electrons passed through the crystal. The 30-MeV electron beam from the microtron passed through a titanium foil of an output microtron flange with a thickness of 0.05 mm, impinged on the Si crystal located in the goniometer at a distance of ~10–15 cm from the output flange, and was scattered in the air. The presence of the foil and the air layer in front of the crystal increased the spread υ_e of the beam from ~0.2 to ~20 mrad.

Bremsstrahlung produced in the Ti foil and the crystal passed through the metal foil and was recorded by a dosimeter (D). A Si crystal with a diameter of 40 mm and a thickness of 0.23 mm was used in the experiment. The ⟨111⟩ axis coincided with the normal to the target surface to an accuracy of at least several fractions of a degree. The crystal was initially located perpendicularly to the electron-beam direction with an error of at most 5°–7°; in this case, the (110) plane was located horizontally with an error of 4°–6°. The radiation scattered in the target (a metal plate) was recorded by an X-ray NaI(Tl) spectrometer with a diameter of 40 mm and a thickness of 1 mm located at an angle of 90° with respect to the direction of the photon beam. To suppress the background, we used a lead spectrometer shielding with a wall thickness of 15 cm. The distance from the target to the operating detector volume was ~80 cm.

In our experiment, we studied the dependence of the readings of the X-ray NaI(Tl) detector recording scattered γ radiation from the thin metal target on the target material and the crystal orientation. Figure 5 shows the smoothed radiation spectra for the Nb target with dimensions of 80 × 150 mm and a thickness of 0.4 mm; they were measured by the detector during the same time (5 min). To operate in the regime of spectral measurements, we decrease the accelerator current from 5 mA (a dose power of ~20 Sv/s) to ~0.5 μA (a dose power of ~2–3 μSv/h), which provided a detector loading of ~1 Hz at an accelerator frequency of 10 Hz.

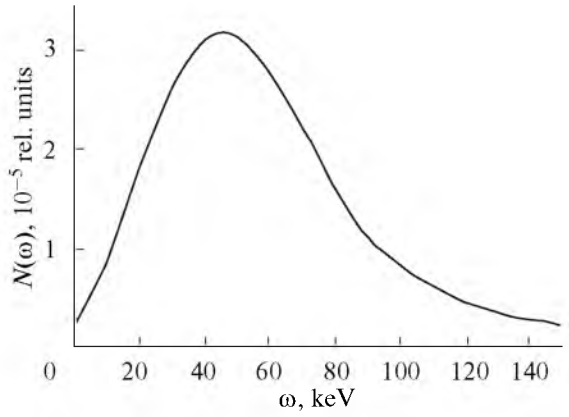

Fig. 6. Model spectrum of radiation entering the detector for bremsstrahlung scattering in the air.

It can be seen from the figure that, along with the Nb CXR peak ($\omega \approx 16.6$ keV), there is radiation with the energy $\omega \sim 70$–100 keV and the yield of this radiation in the experiments with and without the target turns out to be approximately the same. The presence of "false" peaks in the spectra is due to the low statistics (the total number of events is ~300–400). Blocking the scattered radiation path with a Pb plate with a thickness of 1 mm added Pb CXR photons with $\omega \sim 70$ keV (dependence *3*) and cut this radiation off almost completely; i.e., this is radiation of the bremsstrahlung beam recorded by the detector.

It is most probable that the appearance of such amplitudes in the recorded radiation spectrum is due to coherent and incoherent scattering of photons of the γ radiation beam from the crystal and Ti foil by the air layer traced by the detector. For a distance of 2 m from the crystal to the target and our Ti and Si targets located in the path of the microtron electron beam, the transverse size of the γ radiation beam is on the order of 40 cm at the target location place. The longitudinal size of the region from which scattered radiation can enter the detector is also of several tens of centimeters, i.e., considerably greater than the operating part of the metal target. Therefore, the contribution of scattered Compton photons is sufficiently large.

To verify this assumption, we simulated the radiation spectrum recorded by the scattered radiation detector in the case in which the γ radiation beam from the Si crystal propagates in the air under the conditions of our experiment. The angle of bremsstrahlung beam collimation was 100 mrad. The same procedure and simulation conditions, as in the preceding section, were used. The smoothed spectrum obtained as a result of simulation is shown in Fig. 6.

It can be seen from this figure that the shape of the scattered radiation spectrum obtained as a result of simulation is sufficiently close to that of the experimental spectrum; i.e., this is a peak with a maximum in the range of 50–60 keV. The decrease in the low-energy region is due to radiation absorption in the bremsstrahlung targets and the air, and that in the hard-photon region is related to a decrease in the efficiency of the thin NaI(Tl) detector as the photon energy increases.

There is no total coincidence. Because we were only interested in the physical nature of the recorded radiation, in our simulation, we did not take the scatter of bremsstrahlung-beam photons into account and assumed that the photon beam having no linear dimensions scatters in the air. The inclusion of these factors must lead to an increase in the effective detector thickness and, consequently, to an increase in the efficiency of hard-photon recording, i.e., to a shift of the maximum of the model spectrum to the large energy range. In addition, it should be mentioned that, because of the small statistics, the shape of the experimental spectrum is determined insufficiently precisely. We can hope that using sufficiently simple measures—for example, a wide-spacing collimator—decreases the air portion controlled by the detector and increases the fraction of CXR photons.

As was mentioned above, the spectrometric and counting operation regimes of the detecting equipment cannot be used to orient the crystal, first of all, because of large time consumption. As the current increases, the number of photons entering the detector increases sharply and a wide pulse produced by the overlap of signals from different photons and by the integration of these signals at the output resistance is observed. To provide the integral regime used to obtain information from the detector, a device synchronized with the acceleration cycle and integrating this signal was designed [33]. After the acceleration cycle was over, the signal from the integrator was measured by an analog-to-digital converter made in the CAMAC standard.

The measurements showed that the microtron current changes within the limits of 20–30% in an uncontrollable way. Because the expected change in the radiation yield as a function of the crystal orientation is of the same order, it is necessary to measure the current during each acceleration cycle with an error of at most 1%. For this purpose, we used a NaI(Tl) detector with a larger size also operating in the integral regime and recording backscattered radiation from the burial, to which bremsstrahlung produced in the crystal was directed. It is well known that the soft component of the primary beam is absorbed in the burial because of the photoeffect and backscattered radiation forms mainly because of Compton scattering of photons with energies larger than several megaelectronvolts and bremsstrahlung of scattered electrons and positrons formed in the burial as a result of the pair creation process [34]. Therefore, for the electron energy $E_0 = 30$ MeV, the total energy of this radiation must not depend strongly on the crystal orientation.

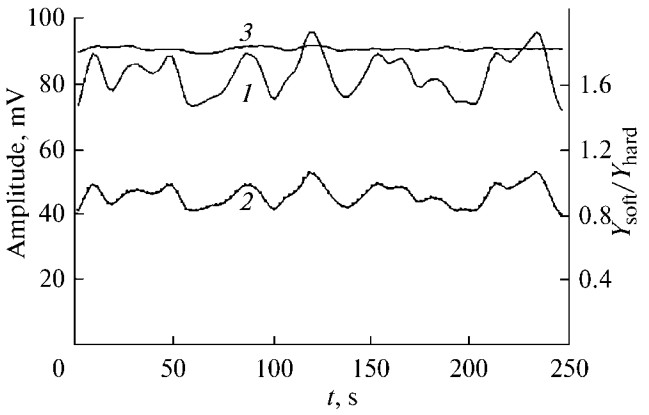

Fig. 7. Dependence of the amplitudes of the X-ray and background detector signals on the time and the ratio of these signals: (*1*) the readings of the scattering radiation detector, (*2*) the readings of the background radiation detector, and (*3*) the ratio of the detector readings.

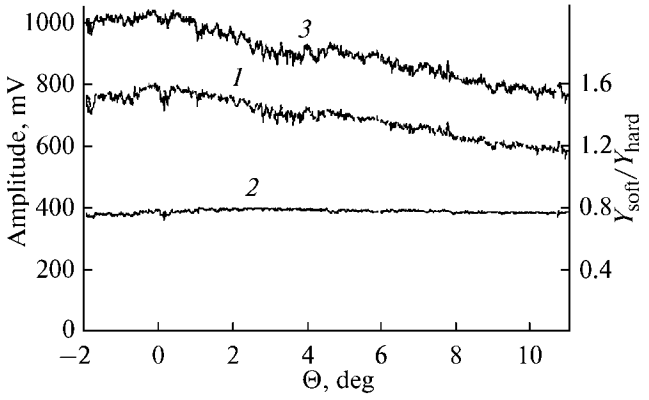

Fig. 8. Orientation dependence of the radiation yield for an electron energy of 30 MeV and Si crystal: (*1*) the readings of the scattering radiation detector, (*2*) the readings of the background radiation detector, and (*3*) the ratio of the detector readings.

Figure 7 shows the dependence of the signal amplitudes recorded by each detector and their ratio for the same crystal orientation. It can be seen from this figure that spontaneous current oscillations of the accelerator lead to a change in the recorded signal amplitudes by 30–40%, while a change in the ratio of amplitudes does not exceed ±1%. Because the expected PXR yield is ~10^{-8}–10^{-7} photon/electron, the same method for measuring the microtron current can be used in the measurements of the angular distributions and orientation dependences of the PXR yield. The sensitivity of this method is insufficient in the measurements of the channeling radiation spectra.

The developed complex of experimental equipment makes it possible to measure dependences of the scattered radiation yield on the crystal orientation. Figure 8 shows the orientation dependence measured with a step of 0.02°. A Pb target with dimensions of 80 × 15 mm and a thickness of 60 μm was located in the radiation path. Each point of the orientation dependence corresponds to 20 acceleration cycles (2 s). The total number of points is 1000, and the measurement time is 37 min. It would take 100 h to obtain the same number of points and to register photon counts or radiation spectra with a statistical error of 5%.

It can be seen from the figure that, as the crystal rotation angle changes, the scattered radiation yield increases gradually, reaching a maximum, and then begins to decrease rapidly. We can see that a second peak for a disorientation angle of ~4° appears. As was shown above (Fig. 7), the measurement error of the ratio of the soft and hard photon yields does not exceed 1–2%; therefore, this maximum is statistically reliable. However, there are no expected narrow peaks attributed to planar channeling radiation of electrons in silicon. The absence of these peaks is more probably due to two reasons. First, the spread of the electron beam $\upsilon_e \sim 20$ mrad is considerably larger than the planar channeling angle $\upsilon_c \sim 1$, because there is foil at the output flange and air in front of the crystal. The second reason is the large contribution of photons scattered in the air. As was mentioned in the discussion of the result of measuring the scattered radiation spectra, the dimensions of the radiation beam registered by the detector are much larger than those of the metal target; therefore, the contribution of the CXR photons to which the expected registration of channeling radiation is related is small.

The recorded dependence of the detector readings on the crystal orientation is due to an increase in the yield of coherent bremsstrahlung photons [35] as the angle between the directions of the crystallographic axis and the electron beam decreases. For the electron energy E_0 = 30 MeV, the energy of coherent bremsstrahlung photons can change from several hundreds of kiloelectronvolts to several megaelectronvolts as a function of the angle between the electron momentum and the crystallographic planes; i.e., it may belong to the energy range for which the Compton scattering cross section is sufficiently large. To confirm the preceding, we present the model dependence on the crystal orientation for scattering of the beam of coherent bremsstrahlung photons in the air (Fig. 9). It was calculated according to the procedure that was used to simulate the dependence of the detector response on the thickness of the metal target. The coherent bremsstrahlung spectra were calculated using the procedure given in [36] for the angle of ⟨111⟩-axis disorientation $\Theta_h = 6.5°$ and for the azimuthal angle of (110)-plane rotation $\varphi = 5°$.

It can be seen from the figure that model orientation dependence has approximately the same shape as the experimental one. We can single out two broad peaks, one of which is higher than the other. As in the

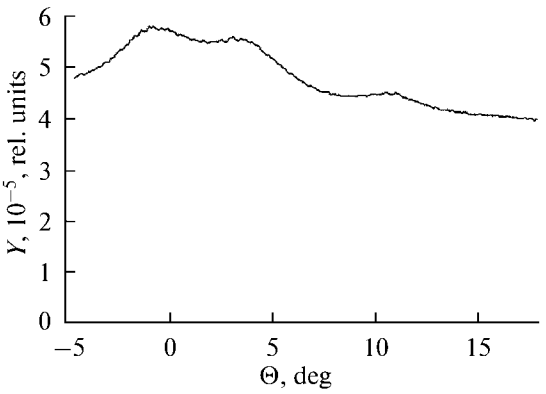

Fig. 9. Model orientation dependence of the detector readings due to the mechanism for coherent bremstrahlung electron scattering in the air.

case of the simulation of scattered radiation spectra, there is no complete agreement between the experimental and calculated dependences. Nevertheless, as was mentioned above, the contribution of the air to the detector readings can be decreased, as a minimum, by one order of magnitude if sufficiently simple measures are used. In this case, peaks attributed to channeling radiation can be recorded with confidence.

CONCLUSIONS

An indispensable minimum of the required equipment, our estimates, and test measurements make it possible to hope that our proposed studies will be accomplished successfully after a scattering chamber connected to the vacuum system of the accelerator is fabricated and installed. In the first stage, we will definitely verify the proposed method for the crystal orientation using the scattered radiation yield, determine whether the fulfillment of the diffraction conditions affects the channeling radiation yield, and measure the angular and orientation dependences of the PXR yield under channeling conditions.

ACKNOWLEDGMENTS

This work was partially supported by the Russian Foundation for Basic Research (grant no. 05-02-17648) and by the Program for Internal Grants of Belgorod State University.

REFERENCES

1. V. G. Baryshevskii and I. Ya. Dubovskaya, Dokl. Akad. Nauk SSSR **231**, 1335 (1976) [Sov. Phys. Dokl. **21**, 741 (1976)].
2. V. G. Baryshevsky and I. Ya. Dubovskaya, Phys. Stat. Solidi B **82**, 403 (1977).
3. V. G. Baryshevskii, O. T. Gradovskii, and I. Ya. Dubovskaya, Vestn. Akad. Nauk BSSR, Ser. Fiz. Mat. Nauk, No. 6, 77 (1987).
4. S. A. Vorob'ev, B. N. Kalinin, S. Pak, and A. P. Potylitsyn, Pis'ma Zh. Eksp. Teor. Fiz. **41**, 3 (1985) [JETP Lett. **41**, 1 (1985)].
5. A. N. Aleinik, A. N. Baldin, E. A. Bogomazova, et al., Pis'ma Zh. Eksp. Teor. Fiz. **80**, 447 (2004) [JETP Lett. **80**, 393 (2004)].
6. V. G. Baryshevskii and I. Ya. Dubovskaya,in *Results of Sci. and Tech., Ser. Beams of Carged particles and Solids* (VINITI, Moscow, 1991), Vol. 4, p. 129 [in Russian].
7. O. V. Bogdanov, K. B. Korotchenko, and Yu. L. Pivovarov, Pis'ma Zh. Eksp. Teor. Fiz. **85**, 684 (2007) [JETP Lett. **85**, 555 (2007)].
8. T. Ikeda, Y. Matsuda, H. Nitta, and Y. H. Ohtsuki, Nucl. Instrum. Methods. Phys. Res. B **115**, 380 (1996).
9. Y. Matsuda, T. Ikeda, H. Nitta, and Y. H. Ohtsuki, Nucl. Instrum. Methods. Phys. Res. B **115**, 396 (1996).
10. R. Yabuki, H. Nitta, T. Ikeda, and Y. H. Ohtsuki, Phys. Rev. B **63**, 174112 (1741).
11. A. N. Baldin, I. E. Vnukov, and R. A. Shatokhin, Pis'ma Zh. Tekh. Fiz. **33**, 87 (2007) [Tech. Phys. Lett. **33**, 625 (2007)].
12. J. U. Andersen and E. Laesgaard, Nucl. Instrum. Methods Phys. Res. B **33**, 11 (1988).
13. K. Yu. Amosov, I. E. Vnukov, B. N. Kalinin, et al., Pis'ma Zh. Eksp. Teor. Fiz. **55**, 587 (1992) [JETP Lett. **55**, 612 (1992)].
14. A. N. Baldin, I. E. Vnukov, B. N. Kalinin, and E. A. Karataeva, Poverkhnost', No. 4, 72 (2006).
15. J. Freudenberger, H. Genz, V. V. Morokhovskii, et al., Phys. Rev. Lett. **84**, 270 (2000).
16. B. Sones, Y. Danon, and R. C. Block, Nucl. Instrum. Methods. Phys. Res. B **227**, 22 (2005).
17. A. V. Chchagin, V. I. Pristupa, and N. A. Khizhnyak, Phys. Lett. A **148**, 485 (1990).
18. F. Arfelli, Nucl. Instrum. Methods. Phys. Res. B **454**, 11 (2000).
19. V. V. Kaplin, S. R. Uglov, O. F. Bulaev, et al., Nucl. Instrum. Methods Phys. Res. B **173**, 3 (2000).
20. C. K. Gary, A. S. Fisher, R. H. Pantell, et al., Phys. Rev. B **42**, 7 (1990).
21. V. I. Shvedunov, A. N. Ermakov, A. I. Karev, et al., in *Proc. of the Particle Accelerator Conf.* (Chicago, 2001), p. 2596.
22. D. Lackey and R. F. Scwitters, Nucl. Instrum. Methods Phys. Res. **81**, 164 (1970).
23. B. N. Kalinin, E. I. Konovalova, G. A. Pleshkov, et al., Prib. Tekh. Eksp., No. 3, 31 (1985).
24. B. L. Berman, *Electron-Photon Interaction in Dense Media*, NATO Sci. Ser. II Math. Phys. Chem., Ed. by H. Wiedemann (Kluwer Acad., Netherlands, 2002), Vol. 49, p. 7.
25. A. N. Baldin, I. E. Vnukov, D. A. Nechaenko, and R. A. Shatokhin, Vestn. Khar'K. Nats. Univ., Ser. Fiz. **744** (3), 51 (2006).
26. M. J. Berger and J. H. Hubbell, Stand. Rep. NBSIR-87, http://physics.nist.gov/XCOM.

27. A. P. Chernyaev, *Interaction of Ionized Emission with Matter* (Fizmatlit, Moscow, 2004) [in Russian].
28. *Physical Values*, The Handbook, Ed. by I. S. Grigor'ev and E. Z. Meilikhov (Energoatomizdat, 1991, Moscow, 1232) [in Russian].
29. A. F. Akkerman, M. Ya. Grudskii, and V. V. Smirnov, *Secondary Electron Emission Produced from Solids by Gamma Rays* (Energoatomizdat, Moscow, 1986) [in Russian].
30. L. I. Schiff, Phys. Rev. **83**, 252 (1951).
31. K. Yu. Amosov, M. Yu. Andreyashkin, I. E. Vnukov, et al., Izv. Vyssh. Uchebn. Zaved., Ser. Fiz. **34** (6), 70 (1991).
32. R. A. Shatokhin, Skhemotekhnika, No. 6, 45 (2007).
33. D. A. Baklanov, I. E. Vnukov, V. K. Grishin, et al., Preprint Mosc. Gos. Univ. No. 2008-1/837 (Moscow, 2008).
34. I. E. Vnukov, S. A. Vorob'ev, O. Yu. Lobanov, et al., Izv. Vyssh. Uchebn. Zaved., Ser. Fiz. **34** (6), 106 (1991).
35. M. L. Ter-Mikaelyan, *Influence of the Medium on Electromagnetic Processes at High Energies* (Akad. Nauk ARM SSR, Yerevan, 1969) [in Russian].
36. I. E. Vnukov, B. N. Kalinin, and A. P. Potylitsyn, Izv. Vyssh. Uchebn. Zaved., Ser. Fiz. **34** (6), 21 (1991).